A new optimization based approach for push recovery in case of multiple noncoplanar contacts

Darine Mansour*, Alain Micaelli*, Adrien Escande* and Pierre Lemerle**

Abstract—This paper presents a new approach for humanoid push recovery in a generalized noncoplanar multicontact context. Our approach is based on a simplified model and consists in stabilizing the perturbed system while maintaining fixed contacts with the environment or by changing a contact configuration when needed to achieve stabilization. A first step of our strategy chooses the optimal contact to change when needed. A second step stabilizes the system while maintaining fixed contacts, when possible or by calculating the minimum change in the position of the optimal contact, capable of stabilizing the system.

I. INTRODUCTION

This study has been motivated by safety issues at mobile and possibly perturbed workplaces. [1] gives the statistics of accidents that occur in leveled environments of such workplaces. In order to assess safety in perturbed environments such as mobile platforms, tests are usually performed on passive dummies or human subjects, which are respectively non representative and too costly. Therefore, within this context, our objective is to develop new controllers for Virtual Humans (VH) in order to make them react to environmental perturbations in a sufficient realistic and natural way. This paper proposes an approach for disturbance rejection, based on a simplified model, from which we will derive whole body controllers in our future works.

A. Related Work

The addressed problem often named *push recovery* is widely treated in literature. It is mainly based on various stability criteria and on a study of simple models.

The most usual stability criteria are the Zero Moment Point (ZMP) [2], [3] and the Foot Rotation Indicator (FRI) [4]. These criteria however present main limitations as the ZMP deals with coplanar contacts and the FRI requires the existence of one single foot contact. An interesting extension has been proposed for the ZMP in [5], but the Generalized ZMP on a virtual plane is based on an assumption of negligible friction forces. [6] proposes the rate of change of centroidal angular momentum as a general stability criterion and measure. Though the control strategies for stability recapture, using the derived condition of a Zero Rate of change of Angular Moment (ZRAM) about the Center Of Mass (COM), are limited to biped robots with coplanar feet contacts.

*D. Mansour, A.Micaelli and A.Escande are with CEA, LIST, Interactive Simulation Laboratory, 18, route du Panorama, BP6, FONTE-NAY AUX ROSES, F-92265 France `darine.mansour@cea.fr`, `alain.micaelli@cea.fr`, `adrien.escande@cea.fr`

**P. Lemerle is with INRS, Department of Work Equipments Engineering, Rue du Morvan, Vandoeuvre Les Nancy F-54519 France `pierre.lemerle@inrs.fr`

A lot of works on disturbance rejection consider the simple model of Linear Inverted Pendulum (LIP) as in [7], [8], [11] and [9]. Introducing the notion of *Capture Points* and *Capture Regions*, the step to make is analytically calculated in [11], sometimes through the conserved orbital energy formulation, as in [9]. In [8], the authors propose an approach based on predictive control and very similar to [17], with additional objectives for the COM. Some models went beyond the LIP by varying the COM height, as in [10], or adding an inertia about the COM in [9] and [11], in order to recover the balance through a change of angular momentum. Still, all these models are restricted to coplanar feet contacts.

Our work in [12] considers a simple model with multiple non coplanar contacts. It proposes a new approach for disturbance rejection based on the minimization of the COM kinetic energy. A dynamic stability indicator is generated to predict whether the system can be stabilized under fixed contacts configuration. A control for push recovery that deals with a step making, when needed, is introduced.

Some works consider whole body humanoid models to treat push recovery. In [13], the angular and linear momentum are controlled to compensate the perturbation. Even if this control can be extended for noncoplanar contacts, it does not deal with contact change when it can not recover perturbation.

A whole body noncoplanar multicontact model is considered in [15], [14] and [16] for the push recovery study. The model is force controlled [14]. The desired contact forces assuring balance are calculated through a feedback and feedforward controller [15] based on the convergence of the COM to a predefined position. The reference position belongs to a region defined on the basis of biped robots and whose computation holds approximations for a non coplanar feet case. The contact change considered to provide the stability is a foot step and its triggering is defined for bipedal balance. Foot steps are symmetric and based on a Symmetric Walking Controller [16].

B. Scope and contribution

Our main contribution consists in a new approach that allows to dynamically stabilize a three dimensional perturbed system, in the general case of multiple non coplanar contacts. We control our model to satisfy dynamic stability during the stabilization and a static stability at the final state without predetermining the stabilization process. An optimal contact change, not restricted to feet, is also considered when needed. In order to obtain a reasonable computation time, allowing predictive optimizations and future interactive applications, we

based our approach on a simplified model, presented in Fig. 1.

- We first compute an algorithm based on energy minimization for a simple model to choose the optimal contact to change if it is needed to stabilize a perturbed model.
- A stabilization algorithm based on predictive optimization is computed to bring the model to a static equilibrium while maintaining fixed contacts when possible or by calculating the optimal change in the contact chosen by the first algorithm, when needed.

We will describe the simplified model in section II. Section III presents the algorithm that chooses the contact to change, when needed for stabilization. Section IV develops the algorithm that stabilizes the perturbed model by maintaining fixed contacts when possible, or by calculating the optimal contact change for stabilization when needed. Some simulation results followed by a discussion are presented in section V.

II. THE SIMPLE MODEL

The simple model, as in [12], consists of a point mass m at the COM and n noncoplanar contact surfaces. The links between the point mass and the contacts, as well as all element bodies relative to the contacts are massless. We introduce contact torques at each surface contact. In a first approach we assume a zero inertia of the body about the COM. We consider a global frame for the system and n local frames, one for each contact. For each contact i local frame, z axis is normal to the contact surface.
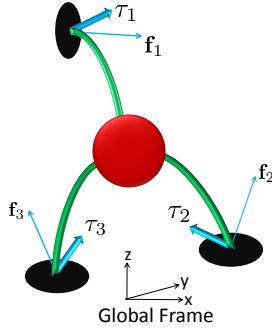

Fig. 1: Simple Model:Point mass and non coplanar contacts

Model parameters and variables are the following:

- Friction coefficient on contact i surface is μ_i
- COM state is $\begin{pmatrix} \mathbf{X} \\ \dot{\mathbf{X}} \end{pmatrix}$ with $\mathbf{X}, \dot{\mathbf{X}} \in \mathbb{R}^3$, expressed in the global frame
- Each contact surface is defined through three components: position of origin $\mathbf{O}_i$ of contact i, $(\mathbf{O}_i \in \mathbb{R}^3)$, normal vector to the contact surface $\mathbf{n}_i \in \mathbb{R}^3$ both expressed with respect to the global frame (See Fig. 1), and S_i, the planar contact area. For sake of simplicity, this surface is linearized to express the belonging to this surface as a linear inequality constraints.

- Each contact i has a reaction wrench of its support $\begin{pmatrix} \mathbf{f}_i \\ \boldsymbol{\tau}_i \end{pmatrix}$ expressed in global frame: $\mathbf{f}_i \in \mathbb{R}^3$ and $\boldsymbol{\tau}_i \in \mathbb{R}^3$ are respectively the contact force and torque.

The model should satisfy physical laws expressed in terms of equality and inequality equations. Equality equations consist of:

$$\begin{cases} m\ddot{\mathbf{X}} &= \sum_i \mathbf{f}_i + m\mathbf{g} \\ \mathbf{0} &= \sum_i [\mathbf{O}_i - \mathbf{X}]\mathbf{f}_i + \sum_i \boldsymbol{\tau}_i \end{cases} \quad (1)$$

with $[.]$ stands here for the skew matrix associated with vector cross product, and $\mathbf{g} = (0,0,-g)^t$ is the gravity vector.

The model should satisfy the second law of Newton (first equation of system (1)).

Since the point mass body has no inertia, the rate of change of angular momentum about the COM is null (second equation of system (1)).

Inequality equations can be built from following conditions:

- The COP the ith contact belongs to S_i.
- To avoid sliding contacts, forces $\mathbf{f}_i$ must belong to friction cones defined by $\|\mathbf{f}_i - (\mathbf{f}_i^t \mathbf{n}_i)\mathbf{n}_i\| \leq \mu_i \mathbf{f}_i^t \mathbf{n}_i$.
- The normal force of the ith contact must be limited to the maximum normal force the contact can admit: $\mathbf{n}_i^t \mathbf{f}_i \leq f_{n_{imax}}$
- To avoid rotational slipping of contacts, the friction torque at the COP of the ith contact is limited proportionally to the contact normal friction force and friction coefficient: $\|\boldsymbol{\tau}_{i_{COP}}\| \leq \alpha \mu_i (\mathbf{n}_i^t \mathbf{f}_i)$

III. ALGORITHM DETERMINING THE CONTACT TO CHANGE WHEN NEEDED

In this section, we propose a strategy that determines the contact to change, if needed to stabilize the model and bring it to a full stop $\dot{\mathbf{X}} = \mathbf{0}$ while satisfying equations (1) and equality and inequality constraints for all contacts.

After an instantaneous perturbation (force impulsion on a short time interval), the system gets an initial COM state $(\mathbf{X}_0, \dot{\mathbf{X}}_0)$. We assume that push implies a negligible initial velocity about z axis. We introduce a time t_r as the time needed to choose the propitious contact to change if it is needed to achieve the stabilization for example by making a step or changing a hand contact. Since $\dot{\mathbf{X}} = \mathbf{0}$ is a desired target for stability, the algorithm consists of minimizing the kinetic energy of the system over t_r while maintaining fixed contacts and while satisfying the equality and inequality constraints. At time t_r, the contact holding the minimum reaction force is the one chosen to move.

A. Discretization

Before we present the algorithm, we discretize system (1) in order to resolve the algorithms numerically, which is a compromise between acceptable computation time and performance. Therefore, we have chosen a simple Taylor series expansion. If $T(s)$ is the time sampling period, and for

$X(t \in]t_k, t_{k+1}])$: $\mathbf{X}_{k^-} = \mathbf{X}_{k^+}$, $\dot{\mathbf{X}}_{k^-} = \dot{\mathbf{X}}_{k^+}$, $\ddot{\mathbf{X}}_{k^+} \neq \ddot{\mathbf{X}}_{k^-}$, and we assume $\frac{d^3\mathbf{X}}{dt}(t \in]t_k, t_{k+1}]) = 0$, we have:

$$\begin{cases} \mathbf{X}_{k+1} &= \mathbf{X}_k + T\dot{\mathbf{X}}_k + \frac{T^2}{2}\ddot{\mathbf{X}}_{k+1} \\ \dot{\mathbf{X}}_{k+1} &= \dot{\mathbf{X}}_k + T\ddot{\mathbf{X}}_{k+1} \end{cases} \qquad (2)$$

B. Strategy determining the changing contact

The strategy deals with fixed contacts and is based on a predictive optimization that minimizes the system kinetic energy over a window h_r with: $t_r = h_r T$ and h_r being a positive integer, while satisfying all constraints for all contacts all over the window. We define a matrix of wrenches expressed in the global frame $\mathbf{W} = \left(\mathbf{W}_1^t \ldots \mathbf{W}_p^t \ldots \mathbf{W}_{h_r}^t \right)^t$ with:

$\mathbf{W}_p = \left(\mathbf{W}_{1p}^t \ldots \mathbf{W}_{ip}^t \ldots \mathbf{W}_{np}^t \right)^t$ and $\mathbf{W}_{ip} = \begin{pmatrix} \mathbf{f}_{ip} \\ \boldsymbol{\tau}_{ip} \end{pmatrix}$ being the support reaction wrench at i^{th} contact for $t \in]t_{p-1}, t_p]$.

1) Formulation of the system over a window:

For $t \in]t_{j-1}, t_j]$ where the positive integer $j \in [1, h_r]$, the system (1) becomes:

$$\begin{cases} m\ddot{\mathbf{X}}_j &= \sum_i \mathbf{f}_{ij} + m\mathbf{g} \\ \mathbf{0} &= \sum_i [\mathbf{O}_i - \mathbf{X}_j]\mathbf{f}_{ij} + \sum_i \boldsymbol{\tau}_{ij} \end{cases} \qquad (3)$$

The first equation of (3) becomes in terms of $\mathbf{W}$:

$$\ddot{\mathbf{X}}_j = \frac{1}{m}\mathfrak{K}_f \mathfrak{K}_\sigma \mathfrak{K}_{(p=j)} \mathbf{W} + \mathbf{g} \qquad (4)$$

where $\mathfrak{K}_f$, $\mathfrak{K}_\sigma$ and $\mathfrak{K}_p$ respectively satisfy $\mathfrak{K}_f \mathbf{W}_{ip} = \mathbf{f}_{ip}$, $\mathfrak{K}_\sigma \mathbf{W}_p = \sum_i \mathbf{W}_{ip}$ and $\mathfrak{K}_{(p=p)} \mathbf{W} = \mathbf{W}_p$.

We replace (4) in the second equation of (2) which we formulate over a window (j) in terms of $\mathbf{W}$:

$$\dot{\mathbf{X}}_j = \dot{\mathbf{X}}_0 + T j\mathbf{g} + \frac{T}{m}\mathfrak{K}_f \mathfrak{K}_\sigma \sum_{u=1}^{j} \mathfrak{K}_{(p=u)}\mathbf{W} \qquad (5)$$

We replace (4) and (5) in the first equation of (2) which we formulate over a window (j) in terms of $\mathbf{W}$:

$$\begin{aligned} \mathbf{X}_j = \quad & \mathbf{X}_0 + T j\dot{\mathbf{X}}_0 + \frac{T^2}{2}\left(\sum_{u=1}^{j} (2(j-u)+1) \right)\mathbf{g} \\ & + \frac{T^2}{2m}\mathfrak{K}_f \mathfrak{K}_\sigma \left(\sum_{u=1}^{j} \left((2(j-u)+1)\mathfrak{K}_{(p=u)} \right) \right)\mathbf{W} \end{aligned} \qquad (6)$$

2) Cost Function:
We consider the following objective:

$$E_c = \frac{1}{2}m\dot{\mathbf{X}}_{h_r}^t \dot{\mathbf{X}}_{h_r} \qquad (7)$$

We use (6) to write this objective function in terms of $\mathbf{W}$. The function we minimize becomes:

$$\arg\min_{\mathbf{W}} (E_c) = \arg\min_{\mathbf{W}} \left(\mathfrak{K}_a \mathbf{W} + \mathbf{W}^t \mathfrak{K}_b \mathbf{W} \right) \qquad (8)$$

with: $\mathfrak{K}_a = 2\mathfrak{K}_1^t \mathfrak{K}_2$ and $\mathfrak{K}_b = \mathfrak{K}_2^t \mathfrak{K}_2$

where: $\mathfrak{K}_1 = \dot{\mathbf{X}}_0 + T h_r\mathbf{g}$ and $\mathfrak{K}_2 = \frac{T}{m}\mathfrak{K}_f \mathfrak{K}_\sigma \sum_{u=1}^{h_r} \mathfrak{K}_{(p=u)}$

3) Equality constraints:
We write them in terms of $\mathbf{W}$ for each time interval $(t \in]t_{j-1}, t_j])$ where j an integer in $[1, h_r]$:

- Zero rate of change of angular momentum (second equation of (3)):
  We replace (6) in the second equation of (3).

$$\begin{aligned} & -\frac{T^2}{2m}\left(\sum_{u=1}^{j-1} ((2(j-1-u)+1)[\mathfrak{K}_{d_u}\mathbf{W}]) \right)\mathfrak{K}_{l_j}\mathbf{W} \\ & + \left(\mathfrak{K}_{c_j} - \mathfrak{K}_{q_j} \right)\mathbf{W} \\ & = \mathbf{0} \ \forall j \end{aligned} \qquad (9)$$

with:

$$\begin{aligned} \mathfrak{K}_{c_j} = \quad & \left(\sum_i \left([\mathbf{O}_i]\mathfrak{K}_f\mathfrak{K}_i \right) + \mathfrak{K}_\tau\mathfrak{K}_\sigma \right)\mathfrak{K}_{(p=j)} \\ & - \left[\mathbf{X}_0 + T(j-1)\dot{\mathbf{X}}_0 \right]\mathfrak{K}_f\mathfrak{K}_\sigma\mathfrak{K}_{(p=j)} \\ & - \frac{T^2}{2}[\mathbf{g}]\mathfrak{K}_f\mathfrak{K}_\sigma\left(\sum_{u=1}^{j-1} \left((2(j-1-u)+1)\mathfrak{K}_{(p=u)} \right) \right) \end{aligned}$$

where: $\mathfrak{K}_i$ is such that $\mathbf{W}_{ip} = \mathfrak{K}_i\mathbf{W}_p$ and $\boldsymbol{\tau}_{ip} = \mathfrak{K}_\tau\mathbf{W}_{ip}$.

$$\begin{aligned} \mathfrak{K}_{q_j} = \quad & -\frac{T^2}{2}[\mathbf{g}]\mathfrak{K}_f\mathfrak{K}_\sigma \sum_{u=1}^{j-1} \left((2(j-1-u)+1)\mathfrak{K}_{(p=u)} \right) \\ & + \frac{T^2}{2}[\mathbf{g}]\mathfrak{K}_f\mathfrak{K}_\sigma\left(\sum_{u=1}^{j-1} (2(j-1-u)+1) \right)\mathfrak{K}_{(p=j)} \end{aligned}$$

$\mathfrak{K}_{d_u} = \mathfrak{K}_f\mathfrak{K}_\sigma\mathfrak{K}_{(p=u)}$ and $\mathfrak{K}_{l_j} = \mathfrak{K}_f\mathfrak{K}_\sigma\mathfrak{K}_{(p=j)}$

- A constant COM height is considered to simplify the problem: $\sum_i f_{ij_z} = mg$. It can be written as:

$$\begin{pmatrix} 0 & 0 & 1 \end{pmatrix}\mathfrak{K}_f\mathfrak{K}_\sigma\mathfrak{K}_{(p=j)}\mathbf{W} = mg \ \forall j \qquad (10)$$

4) Inequality constraints:
As stated above, the system must verify four inequality constraints. We write them in terms of $\mathbf{W}$ for each contact (i) and for each time interval $\left(t \in]t_{j-1}, t_j] \right)$ where j is an integer in $[1, h_r]$:

- Contact forces must belong to friction cones, and in case of four faces discretized cones, we have the following relation in terms of $\mathbf{W}$:

$$\begin{pmatrix} 1 & -1 & \mu_i \\ 1 & 1 & \mu_i \\ -1 & 1 & \mu_i \\ -1 & -1 & \mu_i \end{pmatrix} R_i^t \mathfrak{K}_f\mathfrak{K}_i\mathfrak{K}_{(p=j)}\mathbf{W} \geq \mathbf{0} \ \forall i, j \qquad (11)$$

with the rotation matrix R_i expressing local frame (i) in global frame.

- COP $\mathbf{P}_i$ must belong to surfaces S_i, and in case of polygonal delimitation of S_i, this constraint can be expressed as $A_i\mathbf{p}_i \leq \mathbf{b}_i$, with $\mathbf{P}_i \in S_i$ and $\mathbf{p}_i = \mathbf{O}_i\mathbf{P}_i$, which in turn can be written as (See Appendix A):

$$\left(A_i[\mathbf{n}_i]\mathfrak{K}_\tau - \mathbf{b}_i\mathbf{n}_i^t\mathfrak{K}_f \right)\mathfrak{K}_i\mathfrak{K}_{(p=j)}\mathbf{W} \leq \mathbf{0} \ \forall i, j \qquad (12)$$

- The normal force of contact i must be limited to the maximum normal force $f_{n_{imax}}$ the contact can admit:

$$\mathbf{n}_i^t\mathfrak{K}_f\mathfrak{K}_i\mathfrak{K}_{(p=j)}\mathbf{W} \leq f_{n_{imax}} \ \forall i, j \qquad (13)$$

TABLE I: Algorithm determining the changing contact

Algo 1	
Given	$\mathbf{O}_i, \mathbf{n}_i, \mu_i, m, (\mathbf{A}_i, \mathbf{b}_i), f_{ni_{max}}$ Initial COM state: $(\mathbf{X}_0, \dot{\mathbf{X}}_0)$
1. **Find W** minimizing COM kinetic energy (8) while satisfying (9), (10), (11), (12), (13) and (14) 2. **Choose** the contact v to move among all contacts i as the one having minimum $\|f_{ih_r}\| = \left\|\mathfrak{K}_f \mathfrak{K}_i \mathfrak{K}_{(p=h_r)} \mathbf{W}\right\|$, index $i \in \{1 \cdots n\}$	

- The norm of the friction torque at the COP $\mathbf{P}_i$ is related to the contact normal friction force and friction coefficient as follows (See Appendix VI-B):

$$\left(\Lambda_1 R_i^t \mathfrak{K}_\tau - \alpha \Lambda_2 \mathbf{n}_i^t \mathfrak{K}_f\right) \mathfrak{K}_i \mathfrak{K}_{(p=j)} \mathbf{W} \leq \mathbf{0} \ \forall i,j \qquad (14)$$

5) Strategy description: The procedure determining the changing contact is summarized in Table I. The predictive optimization generates **W** minimizing the cost function and satisfying all constraints. The problem is solved by using a non linear optimization method (interior-point). The objective and constraint gradient functions are calculated in order to decrease the solver computation time.

At time $t_r = Th_r$, the contact v holding the minimum force is chosen to move in case it is needed for stabilization.

IV. STABILIZATION ALGORITHM

In this section, we present the algorithm that stabilizes the system in initial state $(\mathbf{X}_0, \dot{\mathbf{X}}_0)$ by bringing it to a static final state. We assume $(\ 0 \ \ 0 \ \ 1\ )\dot{\mathbf{X}}_0 = 0$. We note that a static state of system (1) is achieved when $\dot{\mathbf{X}} = \mathbf{0}$, $\ddot{\mathbf{X}} = \mathbf{0}$ where equations (1) are satisfied, as well as constant COM height, friction cone, COP, maximum normal force and friction torque conditions for all contacts. The algorithm treats simultaneously a stabilization with fixed contacts and with contact change.

A. Overview of the approach

In a first step, the algorithm considers a stabilization with contact change and we assume the contact change occurs instantly. We fix a stabilization time t_s taken by a human to try to reach a stable static state. The algorithm is based on a predictive optimization that generates the new contact position $\mathbf{O}_v$ that both minimizes the norm of the distance it covers from its initial position $\mathbf{O}_{v_0}$ and assures a static state over a window h_s where $t_s = h_s T$ with h_s being a positive integer, while satisfying all constraints for all contacts all over the window. A static state over a window h_s implies $\dot{\mathbf{X}}_{(h_s-1)} = \mathbf{0}$ and $\ddot{\mathbf{X}}_{h_s} = \mathbf{0}$. At the end of the optimization, if the generated $\mathbf{O}_v$ is different from $\mathbf{O}_{v_0}$, then the contact v should change to the new position $\mathbf{O}_v$ to assure stabilization.

B. Algorithm of Stabilization

We define a vector expressed in global frame $\mathbf{Y} = \begin{bmatrix} \mathbf{W} \\ \mathbf{O}_v \end{bmatrix}$ where $\mathbf{W} = \left(\mathbf{W}_1^t \ldots \mathbf{W}_p^t \ldots \mathbf{W}_{h_s}^t\right)^t$ and matrices $\mathfrak{K}_W$ and $\mathfrak{K}_O$ are defined as $\mathfrak{K}_W \mathbf{Y} = \mathbf{W}$ and $\mathfrak{K}_O \mathbf{Y} = \mathbf{O}_v$.

1) Cost Function: We want to minimize the *distance* that the changing contact covers. We consider the following objective:

$$distance = \|\mathbf{O}_v - \mathbf{O}_{v_0}\|^2 \qquad (15)$$

In terms of **Y**, this objective function is expressed as:

$$\arg\min_{\mathbf{Y}} (distance) = \arg\min_{\mathbf{Y}} \left(-2\mathbf{O}_{v_0}^t \mathfrak{K}_O \mathbf{Y} + \mathbf{Y}^t \mathfrak{K}_O^t \mathfrak{K}_O \mathbf{Y}\right) \quad (16)$$

2) Equality constraints: We write them in terms of **Y** for each time period $\left(t \in \left]t_{j-1}, t_j\right]\right)$ where j an integer in $[1, h_s]$:

- Zero rate of change of angular momentum:
  The fact that $\mathbf{O}_v$ is unknown adds a non linearity to this constraint that becomes:

$$\left(\mathfrak{K}_{r_j} - \mathfrak{K}_{q_j} + [\mathfrak{K}_O \mathbf{Y}]\mathfrak{K}_f \mathfrak{K}_i \mathfrak{K}_{(p=j)}\right)\mathfrak{K}_W \mathbf{Y}$$
$$- \frac{T^2}{2m}\left(\sum_{u=1}^{j-1}\left((2(j-1-u)+1)[\mathfrak{K}_{d_u}\mathfrak{K}_W \mathbf{Y}]\right)\right)\mathfrak{K}_{l_j}\mathfrak{K}_W \mathbf{Y}$$
$$= \mathbf{0} \ \forall j \qquad (17)$$

$$\mathfrak{K}_{r_j} = \left(\sum_{\substack{i=1 \\ i \neq v}}^{n}\left([\mathbf{O}_i]\mathfrak{K}_f \mathfrak{K}_i\right) + \mathfrak{K}_\tau \mathfrak{K}_\sigma\right)\mathfrak{K}_{(p=j)}$$
$$- \left[\mathbf{X}_0 + T(j-1)\dot{\mathbf{X}}_0\right]\mathfrak{K}_f \mathfrak{K}_\sigma \mathfrak{K}_{(p=j)}$$
$$- \frac{T^2}{2}[\mathbf{g}]\mathfrak{K}_f \mathfrak{K}_\sigma \left(\sum_{u=1}^{j-1}\left((2(j-1-u)+1)\mathfrak{K}_{(p=u)}\right)\right)$$

- Constant COM height:

$$(\ 0 \ \ 0 \ \ 1\ )\mathfrak{K}_f \mathfrak{K}_\sigma \mathfrak{K}_{(p=j)}\mathfrak{K}_W \mathbf{Y} = mg \ \forall j \qquad (18)$$

3) Inequality constraints: We write them in terms of **Y** for each contact i and for time period $\left(t \in \left]t_{j-1}, t_j\right]\right)$ where j is an integer in $[1, h_s]$:

- Contact forces in discretized friction cones:

$$\begin{pmatrix} 1 & -1 & \mu_i \\ 1 & 1 & \mu_i \\ -1 & 1 & \mu_i \\ -1 & -1 & \mu_i \end{pmatrix} R_i^t \mathfrak{K}_f \mathfrak{K}_i \mathfrak{K}_{(p=j)}\mathfrak{K}_W \mathbf{Y} \geq \mathbf{0} \ \forall i,j \quad (19)$$

- COP $\mathbf{P}_i$ must belong to linearized S_i:

$$\left(A_i[\mathbf{n}_i]\mathfrak{K}_\tau - \mathbf{b}_i \mathbf{n}_i^t \mathfrak{K}_f\right)\mathfrak{K}_i \mathfrak{K}_{(p=j)}\mathfrak{K}_W \mathbf{Y} \leq \mathbf{0} \ \forall i,j \qquad (20)$$

- The normal force of contact (i) limited to $f_{ni_{max}}$:

$$\mathbf{n}_i^t \mathfrak{K}_f \mathfrak{K}_i \mathfrak{K}_{(p=j)}\mathfrak{K}_W \mathbf{Y} \leq f_{ni_{max}} \ \forall i,j \qquad (21)$$

- The friction torque at the COP $\mathbf{P}_i$ constraint:

$$\left(\Lambda_1 R_i^t \mathfrak{K}_\tau - \alpha \Lambda_2 \mathbf{n}_i^t \mathfrak{K}_f\right)\mathfrak{K}_i \mathfrak{K}_{(p=j)}\mathfrak{K}_W \mathbf{Y} \leq \mathbf{0} \ \forall i,j \qquad (22)$$

TABLE II: Stabilization Algorithm

Algo 2	
Given	$\mathbf{O}_i, \mathbf{n}_i, \mu_i, m, (\mathbf{A}_i, \mathbf{b}_i), f_{ni_{max}}$ Initial COM state: $(\mathbf{X}_0, \dot{\mathbf{X}}_0)$
	1. **Determine** from **Algo 1** the contact v with initial position $\mathbf{O}_{v_0}$, likely to be changed 2. **Find Y** minimizing the distance covered by contact v (16) while satisfying (17), (18), (19), (20), (21), (22), (23), (24) and (25) 3. **If** new contact position $\mathbf{O}_v = \mathbf{O}_{v_0}$ Stabilization successful without contact change **Elseif** $\mathbf{O}_v$ is geometrically reachable by the model The model is stabilized with a contact change from $\mathbf{O}_{v_0}$ to $\mathbf{O}_v$ **Else** Successive contact changes can be envisaged 4. **Compute** the COM trajectory during the the stabilization through $\mathbf{X}_j$ in (6), index $j \in \{1 \cdots h_s\}$ with $\mathbf{W} = \mathfrak{K}_W \mathbf{Y}$

4) Additional Constraints:

- The new contact position $\mathbf{O}_v$ must belong to the surrounding environment. Taking into account non collision constraints, the geometrical zone to which $\mathbf{O}_v$ can belong is linearized and expressed as $C_m \mathbf{O}_v \leq \mathbf{d}_m$, which in turn is expressed in terms of $\mathbf{Y}$ as:

$$C_m \mathfrak{K}_O \mathbf{Y} \leq \mathbf{d}_m \qquad (23)$$

- A condition of a static state over a window h_s is: $\dot{\mathbf{X}}_{(h_s-1)} = \mathbf{0}$. Using (5), we write this constraint in terms of $\mathbf{Y}$:

$$\frac{T}{m} \mathfrak{K}_f \mathfrak{K}_\sigma \left(\sum_{u=1}^{h_s-1} \mathfrak{K}_{(p=u)} \right) \mathfrak{K}_W \mathbf{Y} = -\dot{\mathbf{X}}_0 - T(h_s-1)\mathbf{g} \quad (24)$$

- Another condition of a static state over a window h_s is: $\ddot{\mathbf{X}}_{h_s} = \mathbf{0}$. Using (4), we write this constraint in terms of $\mathbf{Y}$:

$$\frac{1}{m} \mathfrak{K}_f \mathfrak{K}_\sigma \mathfrak{K}_{(p=h_s)} \mathfrak{K}_W \mathbf{Y} = -\mathbf{g} \qquad (25)$$

5) Algorithm description: The stabilization algorithm is summarized in Table II. Similarly to **Algo 1**, the problem is solved by using a non linear optimization method (interior-point). The objective and constraint gradient functions are also calculated in order to decrease the solver computation time. If the generated $\mathbf{O}_v$ is equal to $\mathbf{O}_{v_0}$, then there is no need for contact change to stabilize the system. In the other case, if the generated new contact position $\mathbf{O}_v$ is reachable by the model relatively to its own geometry then the perturbation can be successfully recovered. Otherwise, successive contact changes can be envisaged following the same procedures. The trajectory and velocity of the COM can be computed all over the stabilization process via the wrench vectors of all contacts over the time intervals of window h_s.

V. SIMULATION RESULTS

In this section, we will show the results of **Algo 1** and **Algo 2** applied for the stabilization of two simplified humanoid

TABLE III: Two contact model parameters

Contact position (meter)	$\mathbf{O}_1 = \begin{pmatrix} 0.15 & 0.3 & 0 \end{pmatrix}^t$ $\mathbf{O}_2 = \begin{pmatrix} 0.65 & 0.3 & 0 \end{pmatrix}^t$
Normal to contact surface	$\mathbf{n}_1 = \mathbf{n}_2 = \begin{pmatrix} 0 & 0 & 1 \end{pmatrix}^t$
m (Kg)	60
Maximum admissible normal force	$f_{n_{1max}} = f_{n_{2max}} = mg$
Friction coefficient	$\mu_1 = \mu_2 = \mu_3 = 0.8,\ \alpha = 0.6$
Left and right foot parameters	$d_1 = 0.12$ (meter) $d_2 = 0.26$ (meter) $\theta = 90$ degree

models. We chose a two contact and a three contact models to show the ability of our strategy to deal with multicontact systems and we perturb the models in different environments in order to reveal the asset of our approach to deal with noncoplanarity.

A. Description of models configurations and stabilization environments

- The first model (M2) has two coplanar feet contacts with $\mathbf{O}_1$ and $\mathbf{O}_2$ being respectively the left and right foot contacts. We chose rectangular feet contact surface with a width of d_1 (m), length of d_2 (m) and a θ (degree) orientation about the local z-axis. This model parameters in initial configuration are recapitulated in (Table III) with respect to global frame and shown in Fig. 2a.

  To show the non coplanarity aspect of our approach, we perturb the model and stabilize it in two different environments. The first one (Env_1) consists of the ground (plane with normal vector $\begin{pmatrix} 0 & 0 & 1 \end{pmatrix}^t$ where both feet lay (See Fig. 2a)) and the second (Env_2) consists of the ground with an additional noncoplanar plane (normal vector $\begin{pmatrix} 0 & -1 & 1 \end{pmatrix}^t$ and a point in plane $\begin{pmatrix} 0 & 0.7 & 0 \end{pmatrix}^t$ expressed in global frame) on which a step can be done (See Fig. 3c).

- In order to show a multicontact manipulability aspect, we perturb a second model (M3) that has has two coplanar feet $\mathbf{O}_1$ and $\mathbf{O}_2$ and a hand point contact $\mathbf{O}_3$ pushing on a support. We assert the non coplanarity by choosing a noncoplanar hand support with normal vector $\begin{pmatrix} 0.5 & -0.87 & 0.6 \end{pmatrix}^t$. We chose similar initial contact positions and surfaces for feet as (M2). This model parameters in initial configuration are recapitulated in (Table IV) with respect to global frame and shown in Fig. 4a. We perturb (M3) in the environment (Env_2).

B. Results of the algorithm determining the contact to change

For the initial configuration of M2 and M3, we choose a COM position $\begin{pmatrix} 0.4 & 0.45 & 0.9 \end{pmatrix}^t$ (m) that satisfies static initial stability of both models. We perturb the models(See Tables V and VI). We consider a time $t_r = 0.3(sec)$ necessary to choose the favorable contact to change if needed and a time period of $T = 0.15$(sec) for discretization. After applying **Algo 1** determining the contact to change, we got the results shown

TABLE IV: Three contact model parameters

Contact position (meter)	$\mathbf{O}_1 = \begin{pmatrix} 0.15 & 0.3 & 0 \end{pmatrix}^t$
	$\mathbf{O}_2 = \begin{pmatrix} 0.65 & 0.3 & 0 \end{pmatrix}^t$
	$\mathbf{O}_3 = \begin{pmatrix} 0.4 & 0.7 & 1.2 \end{pmatrix}^t$
Normal to contact surface	$\mathbf{n}_1 = \mathbf{n}_2 = \begin{pmatrix} 0 & 0 & 1 \end{pmatrix}^t$
	$\mathbf{n}_3 = \begin{pmatrix} 0.5 & -0.87 & 0.6 \end{pmatrix}^t$
m (Kg)	60
Maximum admissible normal force	$f_{n_{1max}} = f_{n_{2max}} = mg$ $f_{n_{3max}} = 15g$
Friction coefficient	$\mu_1 = \mu_2 = \mu_3 = 0.8, \ \alpha = 0.6$
Left and right foot parameters	$d_1 = 0.12$ (meter) $d_2 = 0.26$ (meter) $\theta = 90$ degree

TABLE V: Results of Algorithm determining the contact to change for M2

Model	M2 in(Env_1) weakly perturbed	M2 in(Env_1 or Env_2) highly perturbed
$\dot{\mathbf{X}}_0$(m/s)	$(-0.40, 0.40, 0)^t$	$(-1.10, 2.10, 0)^t$
$\mathbf{Force}_{O_1}$(N)	$(31.66, -19.51, 391.19)^t$	$(119.69, 125.25, 588.60)^t$
$\mathbf{Force}_{O_2}$(N)	$(31.73, -22.00, 197.41)^t$	$(0.00, 0.00, 0.0015)^t$
$\mathbf{Force}_{O_3}$(N)	$\cdots$	$\cdots$

in Tables V and VI and illustrated in figures (Fig. 2b, Fig. 3a and Fig. 4b): we show the initial postures of the models with the contact forces resulting from **Algo 1** represented as arrows applied at the COP of each contact at t_r. The force arrows have lengths proportional to real values. They illustrate the force distribution between the contacts at t_r. In both models and for all perturbations, the right foot holds the minimum force, which seems veracious given the direction of perturbation with respect to the models configuration. Thus, the right foot is chosen to change contact in case it is infeasible to stop the models in a static state while maintaining fixed contacts.

C. Stabilization results

We calculate the minimum contact change necessary to bring the models to a full stop in a static state by applying the stabilization algorithm (**Algo 2**) with the right foot ($\mathbf{O}_v = \mathbf{O}_2$) being the contact changing and making a minimum step. We choose a stabilization time $t_s = 0.75$(sec) with a time period of $T = 0.15$(sec). The resulting step and final state are presented in Tables VII and VIII for both models. The results are visualized in figures (Fig.2, Fig.3 and Fig.4) where the purple arrow indicates the direction of perturbation collinear to the COM initial velocity.

TABLE VI: Results of Algorithm determining the contact to change for M3

Model	M3 in Env_2
$\dot{\mathbf{X}}_0$(m/s)	$(-1.54, 2.94, 0)^t$
$\mathbf{Force}_{O_1}$(N)	$(112.69, 130.05, 588.60)^t$
$\mathbf{Force}_{O_2}$(N)	$(-2.24, -1.63, 8.91)^t$
$\mathbf{Force}_{O_3}$(N)	$(72.19, -162.68, -8.91)^t$

TABLE VII: Stabilization results

Model	M2 in Env_1 weakly perturbed	M2 in Env_1 highly perturbed
Final position of right foot COP(m)	$(0.61, 0.53, 0)^t$	$(0.12, 1.01, 0)^t$
Step length(m)	0	0.73
COM final position(m)	$(0.34, 0.54, 0.90)^t$	$(0.12, 0.93, 0.90)^t$
Final $\mathbf{Force}_{O_1}$(N)	$(0, 0, 326.17)^t$	$(-0.37, 1.70, 82.87)^t$
Final $\mathbf{Force}_{O_2}$(N)	$(0, 0, 262.43)^t$	$(0.37, -1.70, 505.73)^t$
Final $\mathbf{Force}_{O_3}$(N)	$\cdots$	$\cdots$

TABLE VIII: Stabilization results

Model	M2 in Env_2	M3 in Env_2
Final position of right foot COP(m)	$(0.27, 0.98, 0.28)^t$	$(0.33, 0.92, 0.22)^t$
Step length(m)	0.61	0.53
COM final position(m)	$(0.21, 0.89, 0.90)^t$	$(0.08, 1.04, 0.90)^t$
Final $\mathbf{Force}_{O_1}$(N)	$(15.89, 121.92, 196.20)^t$	$(4.13, 252.57, 349.85)^t$
Final $\mathbf{Force}_{O_2}$(N)	$(-15.89, -121.92, 392.40)^t$	$(-83.34, -102.67, 247.30)^t$
Final $\mathbf{Force}_{O_3}$(N)	$\cdots$	$(79.21, -149.90, -8.56)^t$

D. Discussion

We presented a new general approach for stabilization of perturbed systems. The novelty remains in the stabilization algorithm and in its general formulation capable to deal with noncoplanarity and with multicontact systems.

The case study in this section reveals the potential of our approach to deal with:

- Non coplanar contacts: a transition from coplanar to non coplanar contacts is possible with M2 in Env_2 and is used to absorb kinetic energy. M3 deals with noncoplanarity during the whole stabilization process.
- Multicontacts: The initial perturbation of M3 in Env_2 is greater than M2 in Env_2. However, the minimum step to stop M3 is smaller than M2. This behaviour is due to the hand contact in (M3) that changes the distribution of forces and plays a crucial role in absorbing kinetic energy (See force distribution of M3 in Env_2 in Table VIII and Fig. 4c).

The stabilization algorithm is efficient in deciding automatically whether a contact change is needed or not: when M2 in Env_1 is weakly perturbed, it is stopped without contact change while a stronger perturbation led to a step(Table VII).

As for the ability of the method to deal with different environments, it is justified in the behaviour of M2: for the same perturbation, a stabilizing minimum step is generated in Env_1 as well as Env_2.

Another asset of our approach is revealed by an acceptable computation time. We will give an idea for the algorithm coded
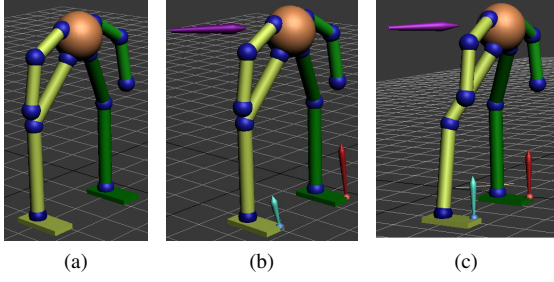
(a)   (b)   (c)

Fig. 2: Graphical stabilization results for M2 weakly perturbed: M2 in initial state (a), M2 in initial state with force vectors (arrows) at COP of contacts at time t_r (b) and M2 stabilized in Env_1 (c).The brown sphere is the COM, the green and yellow elements refer respectively to the left and right part of the model body.The purple arrow indicates the direction of perturbation.
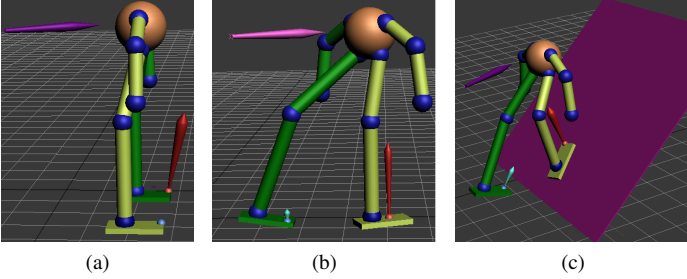

(a)   (b)   (c)

Fig. 3: Graphical stabilization results for M2 highly perturbed: In initial state with force vectors (arrows) at COP of contacts at time t_r (a), M2 stabilized in Env_1 (b) and in Env_2 (c).

in Matlab with a machine of a 2GHz core2 duo processor and 2GB RAM.

- **Algo 1** takes 1.1966(s) for the (M3) and 0.6896(s) for the (M2), both perturbed in Env_2.
- **Algo 2** takes 40.5698(s) for (M3) and 15.7527(s) for (M2), both perturbed in Env_2.

Some choices and heuristics are considered in our approach:

- The choice of t_r and t_s values in the result section is heuristic. We will refine them through later experiments we will lead on human subjects.
- We determine the contact likely changing by assuming it is the one supporting the weaker contact forces after t_r. The choice of the contact can be more complex. We will search for rules helping to enhance it, based on a priori knowledge or experience.

Our approach is based on a simple model. In our ongoing and future work, we will improve it by adding inertia about the COM and by making use of the angular momentum in the process of disturbance rejection.

For a real-time context, our method is still time consuming, but it can serve as a training for learning control as in [18].

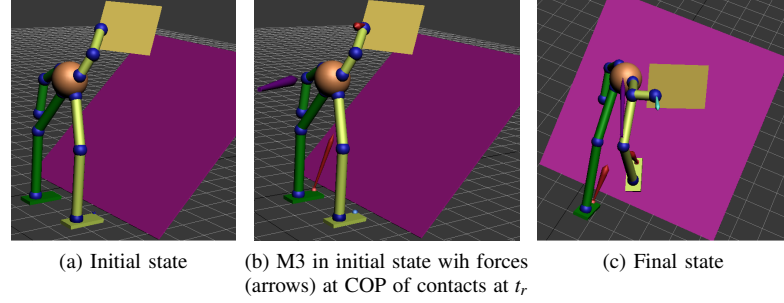In order to achieve realistic human reactions to perturbations, a next step of our work consists in deriving from our method a whole body controller for Virtual Manikins, still keeping our simple model as a reference.

Finally, we will evaluate our approach by comparing it to human reactions to perturbations, through experiments led on human subjects.

VI. APPENDIX

A. Expression of COP Constraint as Local Wrench Constraint

Consider:

- Surface S with a frame based in $\mathbf{O} \in S$;
- COP point $\mathbf{P} \in S$ and $\mathbf{OP} = \mathbf{p}$;
- Normal vector $\mathbf{n}$ to S;
- Wrench $\mathbf{W} = \begin{pmatrix} \mathbf{f} \\ \tau \end{pmatrix}$ applied on S by environment;
- A linear constraint on COP: $\mathbf{Ap} \le \mathbf{b}$.

subscript i has been omitted here for a simpler formulation.

Transporting wrench $\mathbf{W}$ at point $\mathbf{P}$ gives wrench $\mathbf{W}_P$ such that:

$$\mathbf{W}_P = \begin{pmatrix} \mathbf{f}_P \\ \tau_P \end{pmatrix} = \begin{pmatrix} \mathbf{f} \\ -[\mathbf{p}]\mathbf{f} + \tau \end{pmatrix} \qquad (26)$$

then, as τ_P and $\mathbf{n}$ must be collinear at COP $\mathbf{P}$, we have:

$$[\mathbf{n}]\,\tau_P = -[\mathbf{n}]\,[\mathbf{p}]\,\mathbf{f} + [\mathbf{n}]\,\tau = 0 \qquad (27)$$

As $[\mathbf{n}]\,[\mathbf{p}] = \mathbf{p}\mathbf{n}^t - (\mathbf{p}^t\mathbf{n})\,I_3$, then:

$$-(\mathbf{n}^t\mathbf{f})\,\mathbf{p} + [\mathbf{n}]\,\tau = 0 \qquad (28)$$

which, combined with constraint $\mathbf{Ap} \le \mathbf{b}$, gives:

$$\mathbf{A}\,[\mathbf{n}]\,\tau - \mathbf{b}\mathbf{n}^t f \le 0 \qquad (29)$$

finally, we get:

$$\left(\mathbf{A}\,[\mathbf{n}]\,\mathfrak{K}_\tau - \mathbf{b}\mathbf{n}^t\mathfrak{K}_f\right)\mathbf{W} \le 0 \qquad (30)$$

B. Expression of friction torque Constraint as Local Wrench Constraint

In the following, we consider the same elements and notations of VI-A with subscripts i and j omitted for simpler formulation.

To avoid rotational slipping, the friction torque must satisfy the following constraint: $\|\boldsymbol{\tau}_P\| \le \alpha\mu\,(\mathbf{n}^t\mathbf{f})$

(a) Initial state   (b) M3 in initial state wih forces (arrows) at COP of contacts at t_r (c) Final state

Fig. 4: Graphical stabilization results for M3

From (28) and the second equation of (26),we get:

$$\left(\mathbf{n}^t\mathbf{f}\right)\boldsymbol{\tau}_P = \left(\mathbf{n}^t\mathbf{f}\right)\boldsymbol{\tau} + [\mathbf{f}][\mathbf{n}]\boldsymbol{\tau} \qquad (31)$$

As $[\mathbf{f}][\mathbf{n}] = \mathbf{n}\mathbf{f}^t - \left(\mathbf{n}^t\mathbf{f}\right)I_3$, then:

$$\boldsymbol{\tau}_P = \frac{1}{\mathbf{n}^t\mathbf{f}}\mathbf{n}\mathbf{f}^t\boldsymbol{\tau} \qquad (32)$$

which combined with the constraint $\|\boldsymbol{\tau}_P\| \leq \alpha\mu\left(\mathbf{n}^t\mathbf{f}\right)$, gives:

$$\mid \mathbf{n}^t\boldsymbol{\tau} + \frac{1}{\mathbf{n}^t\mathbf{f}}\left(\mathbf{f} - \left(\mathbf{n}^t\mathbf{f}\right)\mathbf{n}\right)^t\left(\boldsymbol{\tau} - \left(\mathbf{n}^t\boldsymbol{\tau}\right)\mathbf{n}\right)\mid \leq \alpha\mu\left(\mathbf{n}^t\mathbf{f}\right) \qquad (33)$$

Since the contraint of belonging of friction forces to friction cones implies:

$$\|\mathbf{f} - \left(\mathbf{n}^t\mathbf{f}\right)\mathbf{n}\| \leq \mu\mathbf{n}^t\mathbf{f} \qquad (34)$$

we have:

$$\mid \mathbf{n}^t\boldsymbol{\tau} + \frac{1}{\mathbf{n}^t\mathbf{f}}\left(\mathbf{f} - \left(\mathbf{n}^t\mathbf{f}\right)\mathbf{n}\right)^t\left(\boldsymbol{\tau} - \left(\mathbf{n}^t\boldsymbol{\tau}\right)\mathbf{n}\right)\mid \leq \mid \mathbf{n}^t\boldsymbol{\tau}\mid + \mu\|\boldsymbol{\tau} - \left(\mathbf{n}^t\boldsymbol{\tau}\right)\mathbf{n}\| \qquad (35)$$

We want:

$$\mid \mathbf{n}^t\boldsymbol{\tau}\mid + \mu\|\boldsymbol{\tau} - \left(\mathbf{n}^t\boldsymbol{\tau}\right)\mathbf{n}\| \leq \alpha\mu\left(\mathbf{n}^t\mathbf{f}\right) \qquad (36)$$

this way, the friction torque constraint (33) is satisfied.
If $\mathbf{n}^t\boldsymbol{\tau} \geq 0$, then (36) becomes:

$$\|\boldsymbol{\tau} - \left(\mathbf{n}^t\boldsymbol{\tau}\right)\mathbf{n}\| \leq \frac{1}{\mu}\left(\alpha\mu\left(\mathbf{n}^t\mathbf{f}\right) - \left(\mathbf{n}^t\boldsymbol{\tau}\right)\right) \qquad (37)$$

which is the equation of a cone that we discretize into four faces and get:

$$\Lambda_3^t R^t \boldsymbol{\tau} \leq \alpha \overbrace{\left(\begin{array}{cccc} 1 & 1 & \cdots \end{array}\right)}^{4}{}^t \left(\mathbf{n}^t\mathbf{f}\right) \qquad (38)$$

with: $\Lambda_3 = \begin{pmatrix} -1 & -1 & 1 & 1 \\ 1 & -1 & -1 & 1 \\ \frac{1}{\mu} & \frac{1}{\mu} & \frac{1}{\mu} & \frac{1}{\mu} \end{pmatrix}$ and R the rotation matrix expressing local frame in global frame.
If $\mathbf{n}^t\boldsymbol{\tau} \leq 0$, then (36) becomes:

$$\|\boldsymbol{\tau} - \left(\mathbf{n}^t\boldsymbol{\tau}\right)\mathbf{n}\| \leq \frac{1}{\mu}\left(\alpha\mu\left(\mathbf{n}^t\mathbf{f}\right) + \left(\mathbf{n}^t\boldsymbol{\tau}\right)\right) \qquad (39)$$

which is also the equation of a cone that we discretize into four faces and get:

$$\Lambda_4^t R^t \boldsymbol{\tau} \leq \alpha \overbrace{\left(\begin{array}{cccc} 1 & 1 & \cdots \end{array}\right)}^{4}{}^t \left(\mathbf{n}^t\mathbf{f}\right) \qquad (40)$$

with: $\Lambda_4 = \begin{pmatrix} -1 & -1 & 1 & 1 \\ 1 & -1 & -1 & 1 \\ \frac{-1}{\mu} & \frac{-1}{\mu} & \frac{-1}{\mu} & \frac{-1}{\mu} \end{pmatrix}$.
Finally we get:

$$\left(\Lambda_1 R^t \mathfrak{K}_\tau - \alpha\Lambda_2 \mathbf{n}^t \mathfrak{K}_f\right)\mathbf{W} \leq \mathbf{0} \qquad (41)$$

with: $\Lambda_1 = \left(\begin{array}{cc} \Lambda_3 & \Lambda_4 \end{array}\right)^t$ and $\Lambda_2 = \overbrace{\left(\begin{array}{ccc} 1 & 1 & \cdots \end{array}\right)}^{8}{}^t$

REFERENCES

[1] C. Gaudez and S. Leclercq, "Accidents de plain-pied. Donnees statistiques nationales et analyses menees en entreprises", *in Jour. of Documents pour le Medecin du Travail*, TF 167, 2008.

[2] M. Vukobratovic and B. Borovac, "Zero-Moment Point- Thrirty five years of his life", *in Int. Jour. of Humanoid Robotics*, Vol. 1, No.1, March 2004, pp. 157-173.

[3] P. Sardain and G. Bessonnet, "Forces Acting on a Biped Robot. Center of Pressure – Zero Moment Point", *in IEEE Trans. on Systems Man & Cybernetics Part A*, Vol. 34, No.5, 2004, pp. 630-637.

[4] A. Goswami, "Foot rotation indicator (FRI) point:A new gait planning tool to evaluate postural stability of biped robots", *in IEEE Int. Conf. on Robotics and Automation*, Detroit, May 1999, pp.47-52.

[5] S. Kagami, K. Nichiwaki, T.Kitagawa, T.Sugihara, M.Inaba and H.Inoue, "A fast generation method of a dynamically stable humanoid robot trajectory with enhancedzmp constraint", *in Proc. 1st IEEE-RAS Int. Conf. on Humanoid Robots*, September 7-8 2000.

[6] A. Goswami and V. Kallem, "Rate of change of angular momentum and balance maintenance of biped robots, *IEEE Int. Conf. on Robotics and Automation*, New Orleans, LA, April 2004.

[7] B. Stephens and C. Atkeson, "Modeling and Control of Periodic Humanoid Balance using the Linear Biped Model", *in International Conference on Humanoid Robots*, Paris, France, 2009.

[8] B. Stephens and C. Atkeson, "Push Recovery by Stepping for Humanoid Robots with Force Controlled Joints",*in International Conference on Humanoid Robots*, Nashville, TN, 2010.

[9] J. Pratt, J. Carff and S. Drakunov, and A. Goswami, "Capture Point: A Step toward Humanoid Push Recovery", *in Proceedings of the IEEE-RAS International Conference on Humanoid Robots*, Genoa, Italy, December 4-6 2006, pp. 200-207.

[10] J. Pratt and S.Drakunov, "Derivation and Application of a Conserved Orbital Energy for the Inverted Pendulum Bipedal Walking Model", *in IEEE International Conference on Robotics and Automation*, April 10-14 2007, pp.4653-4660.

[11] B. Stephens, "Humanoid Push Recovery", *in International Conference on Humanoid Robots*, Pittsburgh, PA, November 2007.

[12] D. Mansour, A. Micaelli and P. Lemerle, "A Computational Approach for Push Recovery in case of Multiple Noncoplanar Contacts", *in Proceedings of IEEE/RSJ International Conference on Intelligent Robots and Systems*, September 25-30 2011, San Francisco, California.

[13] M. Abdallah and A. Goswami , "A Biomechanically Motivated Two-Phase Strategy for Biped Upright Balance Control", *in Proceedings of the IEEE International Conference on Robotics and Automation*, April 18-22 2005, pp. 1996- 2001.

[14] S. Hyon, J. G. Hale, and G. Cheng, "Full-body compliant human-humanoid interaction: Balancing in the presence of unknown external forces", *in IEEE Transactions on Robotics*, Vol.23, No.5, 2007, pp.884-898.

[15] S. Hyon, G. Cheng, "Disturbance Rejection for Biped Humanoids", *in IEEE International Conference on Robotics and Automation*, 10-14 April 2007, pp.2668-2675.

[16] S. Hyon. and G. Cheng, "Passivity-based full-body force control for humanoids and application to dynamic balancing and locomotion", *in Proceedings of IEEE/RSJ International Conference on Intelligent Robots and Systems*, Beijing, China, 2006, pp.4915-4922.

[17] Holger Diedam, Dimitar Dimitrov, Pierre-Brice Wieber, Katja Mombaur, and Moritz Diehl. Online Walking Gait Generation with Adaptive Foot Positioning through Linear Model Predictive Control. In *IEEE-RSJ International Conference on Intelligent Robots & Systems*, Nice, France, 2008.

[18] J.Rebula, F.Canas, J.Pratt and A.Goswami, "Learning Capture Points for Humanoid Push Recovery", *in EEE-RAS Int. Conf. on Humanoid Robots*, November-December 2007, Pittsburgh, PA.